Photocatalytic Oxidation of NO x under Visible LED Light Irradiation over Nitrogen-Doped Titania Particles with Iron or Platinum Loading

ARTICLE *in* THE JOURNAL OF PHYSICAL CHEMISTRY C · JANUARY 2008

Impact Factor: 4.77

Photocatalytic Oxidation of NO_x under Visible LED Light Irradiation over Nitrogen-Doped Titania Particles with Iron or Platinum Loading

Shu Yin,*,† Bin Liu,† Peilin Zhang,† Takeshi Morikawa,‡ Ken-ichi Yamanaka,‡ and Tsugio Sato†

Institute of Multidisciplinary Research for Advanced Materials, Tohoku University, 2-1-1, Katahira, Aoba-ku, Sendai, Japan, and Toyota Central R&D Laboratories Inc., Nagakute, Aichi 480-1192, Japan

Received: April 18, 2008; Revised Manuscript Received: May 25, 2008

The photocatalytic deNO_x activities of titania, nitrogen-doped titania, Fe-loaded nitrogen-doped titania, and Pt-loaded nitrogen-doped titania under irradiation from monochrome LED lamps using various light wavelengths were investigated in detail. The improvement of visible light induced photocatalytic activity was successfully realized using Fe and Pt loading. Both Fe-loaded nitrogen-doped titania and Pt-loaded nitrogen-doped titania showed excellent visible light response ability. The photocatalytic activity exhibited by Pt- loaded nitrogen-doped titania was several times higher than that of nitrogen-doped titania under the visible light irradiation of $\lambda = 627$ and 530 nm. The relationship between photocatalytic activity and irradiation light wavelength was investigated in detail. The relationship between the intensity of low-level chemiluminescence generated by singlet oxygen ($^1O_2$) and photocatalytic activity was also discussed.

1. Introduction

Photocatalysis has been becoming an increasingly attractive method for both atmosphereric and aquatic purification. The photocatalytic destruction of NO is of great significance from a practical application viewpoint because NO is one of the most common pollutants found in exhaust emissions from automobiles. In 2004, a Japanese industrial standard (JIS standard) for photocatalytic deNO_x reaction was established.[1] According to this standard, it is recommended that the activity of a photocatalyst should be characterized through measurement of the decrease in concentration of NO at the outlet of a continuous reactor. Yield products such as HNO_2 and HNO_3 absorbed on the surface of a photocatalyst may lead to the decrease of photocatalytic activity after an extended period of operation. The regeneration of a photocatalyst may be accomplished by washing with water. It is clear that the photocatalytic decomposition of NO is very important in practical applications. Up to this point, usually 100−500 W high pressure mercury lamps were used as light sources in photocatalytic studies.[2–4] Few studies related to low-visiblility light irradiation with monochrome LEDs were carried out. Although many kinds of photocatalysts have been developed, titania remains the most effective and, through light irradiation, can be applied to the decomposition of many pollutive substances, such as nitrogen monoxide and other atmospheric and aquatic volatile organic compounds (VOC). On the other hand, titania can only be encouraged by UV light because of its large band gap value of ca. 3 eV. In order to utilize this solar energy effectively, it is necessary to develop a visible light reactive photocatalyst. In 2001, Asahi et al.[5,6] reported that nitrogen-doped titanium oxide ($TiO_{2-x}N_x$) with high visible light photocatalytic activities could be prepared either by sputtering TiO_2 into an N_2 (40%)/Ar gas mixture followed by annealing in N_2 gas at 550 °C, or by treating anatase TiO_2 powder in the NH_3 (67%)/Ar atmosphere at 600 °C. It was also pointed out that nitrogen doping leads to a narrowing of the band gap through formation of an N 2p state above the O 2p state. This consequently induces visible light responsive photocatalytic activity. It was also predicted that other kind of anions such as C, S, and F would cause a similar effect to that of nitrogen. Since then, many researchers have focused much of their attention on anion-doped photocatalysts.[7–16] However, few studies were carried out on the $TiO_{2-x}N_x$ photocatalyst when modified with transition metals. It has been reported that copper ion doping has a positive effect on the enhancement of $TiO_{2-x}N_x$ photocatalytic activity used for acetaldehyde oxidation.[17] It is also reported that the sensitization of photocatalytic activity produced by S- or N-doped TiO_2 particles can be accomplished through the absorption of Fe^{3+} cations.[18] Iron and platinum loading is expected to improve both the effectiveness of the charge transfer as well as the visible light induced photocatalytic activity.[19] Aside from anion- and cation-doping, it has been accepted that photocatalytic activity is also strongly related to crystallinity as well as the specific surface area of a prepared powder.[2] Well-crystallized photocatalysts with a fine particle size usually exhibit excellent photocatalytic activity. Some solution processes such as hydrothermal and solvothermal processes have been utilized for the synthesis of well-crystallized nanosize photocatalysts with high photocatalytic activity.[14,20] Normally in photocatalytic research, titania photocatalytic reactions are mainly generated from the exertions of hydroxyl radicals (OH•) and superoxide radicals (O_2•).[21–23] Singlet oxygen ($^1O_2$) is also an active oxygen species whose reactivity has been known as a strong oxidation reagent for organic compounds.[24,25] However, regarding the reaction mechanism of titania photocatalysis, $^1O_2$ has been ignored for some reason.[22,24] There have been, however, very few reports predicting the formation of $^1O_2$ in titania photocatalytic systems. In the present research, the photocatalytic deNO_x activities of titania, nitrogen-doped titania, Fe-loaded nitrogen-doped titania, and Pt-loaded nitrogen-doped titania under irradiation of monochrome LED lamps with various light wavelengths were

* To whom correspondence should be addressed. E-mail: shuyin@tagen.tohoku.ac.jp.
† Tohoku University.
‡ Toyota Central R&D Laboratories Inc.

10.1021/jp803371s CCC: $40.75
Published on Web 07/16/2008

investigated in detail. The relationship between irradiated light wavelengths and the photocatalytic activity of Fe- or Pt-loaded $TiO_{2-x}N_y$ was investigated. The relationship between low-level intensity chemiluminescence generated from singlet oxygen ($^1O_2$) and the photocatalytic activity was also discussed.

Experimental Section

The bare $TiO_{2-x}N_x$ (denoted as TiON) powder samples were prepared by treating anatase TiO_2 powder (ST-01, Ishihara Sangyo Kaisha, Osaka, Japan) in an NH_3 atmosphere at 600 °C for 3 h, followed by annealing at 300 °C for 2 h in humid air. Concentrations of nitrogen were found to be about 0.25 at. %, as observed with X-ray photoelectron spectroscopy (XPS). As a comparative sample, the anatase TiO_2 powder ST-01 was heat-treated in air at 500 °C for 1 h (denoted as S-TiO_2). The BET specific surface areas of the TiON and S-TiO_2 powders were 57.7 and 100.7 m^2/g, respectively. The powder was composed of anatase particles with average diameters of about 20 nm. Fe and Pt loading was performed by dispersing $TiO_{2-x}N_x$ powder in a nitric acid aqueous solution containing $Fe(NO_3)_3$ (Wako Pure Chemical Industries Ltd., Osaka, Japan) and $Pt(NH_3)_2(NO_3)_2$ (Tanaka Kikinzoku Kogyo K.K., Tokyo) at room temperature, followed by stirring for 1 h and then heating at 150 °C to encourage water evaporation. Finally, the Fe- and Pt-loaded catalysts were calcined at 300 and 400 °C for 2 h, respectively. The amount of loaded species was 0.5 wt% for both Fe and Pt. The samples loaded with Fe and Pt were denoted as TiONFe and TiONPt, respectively.

The phase constitution of the products was determined using X-ray diffraction analysis (XRD, Shimadzu XD-D1), and its composition was analyzed using an energy dispersive X-ray spectrometer (EDX-800HS, Shimadzu). The BET specific surface area was determined from the amount of nitrogen adsorption at 77 K (Quantachrome, NOVA 4200e). The primary particle size was determined by Sherrer's equation from the half-width of the (101) peak of titania. The agglomerated secondary particle size d_{50} was determined by a laser diffraction particle size analyzer (Shimadzu SALD-7000). Photocatalytic activity during the oxidative destruction of nitrogen monoxide was determined by measuring the concentration of NO gas at the outlet of the reactor (373 cm^3) during photoirradiation by a constant flow of 1 ppm NO−50 vol.% air (balanced N_2) mixed gas (200 cm^3 min^{-1}). The photocatalyst sample was placed in a hollow 20 mm in length, 16 mm in width, and 0.5 mm in depth on a glass holder plate and set in the bottom center of the reactor. Light wavelength was controlled by selecting various types of LED lamps (OptiLED, SP-E27, 2.5 W) with different light wavelength distributions. The light wavelength distribution spectra of the LED light sources were measured using a multichannel spectrophotometer (JASCO, MD-100). Figure 1 shows the wavelength distributions of various LED lamps. All of the LED lamps showed narrow light wavelength distributions, meaning that almost any monochromatic light, from near UV light to visible light (red, green, blue, etc.), could be produced. Photocatalytic characterizations were carried out using different LED lamps at the same light irradiation intensity of 2 mW on the sample surfaces by controlling the distance between the lamps and surfaces. The low-level chemiluminescence intensity of singlet oxygen ($^1O_2$) was measured using a multiluminescence spectrometer (MLA-GOLDS; Tohoku Electric Ind., Japan) at 25 °C in air or in 1 ppm NO−50 vol.% air (balanced N_2) mixed gas atmosphere. Approximately 1.2 g of the sample was placed in a stainless steel sample chamber (50 mm in diameter) and irradiated for 5 s with four different types of LED light: UV light (wavelength 375 nm), blue light (wavelength 470 nm), green light (wavelength 530 nm), and red light (wavelength 630 nm). The chemiluminescence intensity of singlet oxygen ($^1O_2$) at a wavelength of 634 nm was measured by subtracting the luminous intensity of $\lambda < 640$ nm from the luminous intensity of $\lambda < 620$ nm using two filters, $\lambda < 620$ nm and $\lambda < 640$ nm.

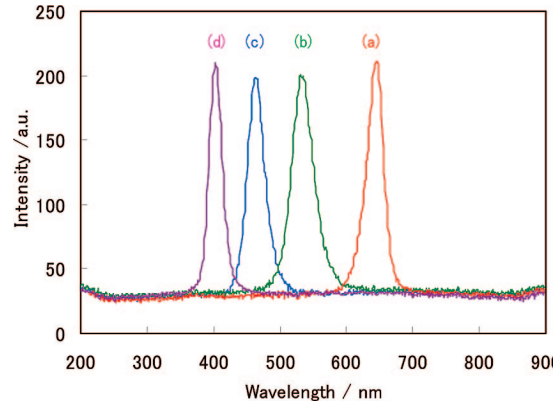

Figure 1. Wavelength distributions of various LED light sources: (a) red light LED, (b) green light LED, (c) blue light LED, and (d) UV light LED.

TABLE 1: Physical Properties of the Prepared Samples

	S-TiO_2	TiON	TiONFe	TiONPt
TiO_2 (%)	100	100	99.5	99.5
Fe_2O_3 (%)	0	0	0.5	0
Pt (%)	0	0	0	0.5
BET specific surface area (m^2 g^{-1})	100.7	57.1	61.1	59.0
d_{BET} (nm)	15.2	26.8	25.1	26.0
d_{XRD} (nm)	34	54	59	55
d_{50} (nm)	76	78	90	90
AF-(50) (d_{50}/d_{XRD})	2.24	1.44	1.52	1.64
mobility (μm cm/V s)	−0.774	−0.902	−0.446	−0.725
ζ-potential (mV)	−9.88	−11.5	−5.69	−9.25

Results and Discussion

Table 1 summarizes the physical properties of the prepared samples. Nitrogen-doped titania samples both with and without metal doping (TiON, TiONFe, TiONPt) showed smaller BET specific surface areas and larger particle sizes than those of undoped titania (S-TiO_2).

Figure 2 shows the XRD patterns of the titania samples. All of the samples possessed the anatase phase, indicating that neither nitrogen doping nor metal loading affected the phase composition of the titania powder. Fe and Pt peaks were not observed since they were present in quite low quantities (see Table 1). The XPS measurement indicated that Pt was composed of a mixture of metallic Pt and PtO, and that Fe was comprised of a mixture of FeO or Fe^{2+} hydroxides on the catalyst surface;[19] the data, however, are not shown here. Table 1 also summarizes the ζ-potentials of the prepared samples. All of the samples showed negative surface charges, with ζ-potentials ranging from about −5.69 to −11.5 mV.

Figure 3 shows the diffuse reflectance spectra of the titania samples. Commercial white titania powder, Degussa P-25, showed a clear absorption edge at around 400 nm, which was related to its band gap energy of about 3 eV. The TiO_2 sample used in the present study, S-TiO_2, showed a DRS spectrum similar to that of P-25. The nitrogen-doped titania samples, however, both with and without metal loading, possessed two-step adsorption spectra. The first may have been related to the

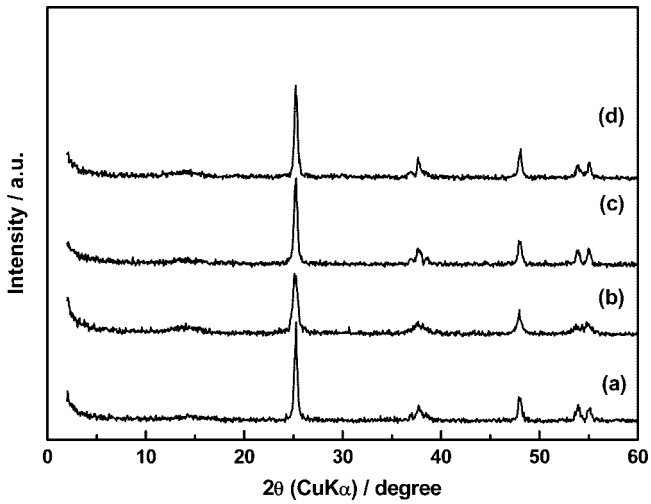

Figure 2. XRD patterns of titania samples: (a) S-TiO_2, (b) TiON, (c) TiONFe, and (d) TiONPt.

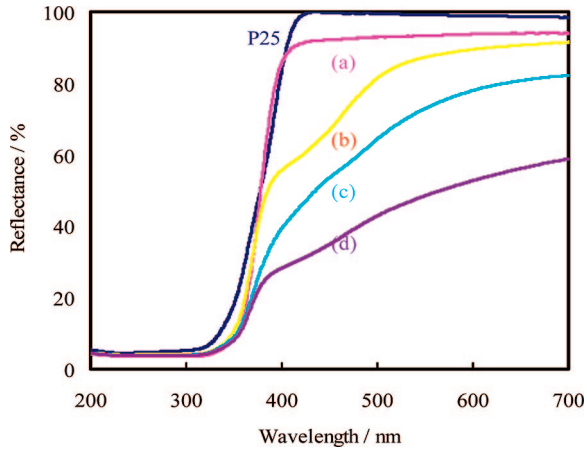

Figure 3. Diffuse reflectance spectra of titania samples: (a) S-TiO_2, (b) TiON, (c) TiONFe, and (d) TiONPt.

original band structure of titania, and the second adsorption (at about 400−650 nm) may have been related to the formation of an N 2p band during nitrogen doping. The samples with Fe or Pt loading showed comparatively deeper colors and greater absorption than that of nitrogen-doped titania over the visible light range 400−700 nm.

Figure 4 shows the irradiation time dependence of the concentration of NO_x in the presence of samples irradiated by various monochromatic LED lamps. In the present study, NO gas was first introduced into the reactor at a steady flow rate of 200 cm^3 min^{-1} before light irradiation. NO_x was then oxidized in a continuous photocatalytic reaction under monochromatic red light irradiation for 10 min until the reaction steadied. Additionally, when the light was turned off, the concentration of NO returned to its initial level of 1 ppm within 10 min, indicating that light energy is essential for the oxidation of nitrogen monoxide. After red light irradiation, the LED lamps were changed in turn to green, blue, and UV light wavelengths. Different samples showed quite different light wavelength dependencies. S-TiO_2 displayed excellent UV light induced activity and very weak photocatalytic activity under blue light irradiation while TiON showed excellent UV light and visible light induced photocatalytic activity. Nitrogen-doped titania, TiON, possessed visible light induced activity under both blue light (445 nm) and green light (530 nm) irradiation. These results are consistent with the DRS spectra in that S-TiO_2 was able to absorb only UV light, while TiON was able to absorb both UV and visible lights. It is notable that the Fe- and Pt-loaded nitrogen titania samples TiONFe and TiONPt showed excellent deNO_x abilities even under red light (627 nm) irradiation. Figure 5A summarizes the data for the different samples under irradiation by lights of various wavelengths. The Pt-loaded sample showed the highest deNO_x abilities in all light wavelength ranges. About 37.8%, 36.8%, 28.2%, and 16.0% of NO_x was removed under continuous irradiation by monochromatic lights 390 nm (UV LED), 445 nm (blue LED), 530 nm (green LED), and 627 nm (red LED) in wavelength, respectively. Previous reports typically used high-pressure 500 W mercury lamps as their photocatalytic reaction light sources. [2–4,10,11,13,14,16] In contrast, in the present research even with the use of very weak monochromatic LED lamps (2.5 W), we successfully induce high deNO_x photocatalytic activity.

Figure 5B,C shows the photoefficiency of the photocatalytic deNO_x reaction and the quantum efficiencies (QEs) of the various samples, respectively. Because all of the samples were irradiated with light of the same intensity, photocatalytic reaction efficiency varied in the same way as photocatalytic activity (Figure 5A). About 0.12−0.24% of the red light (627 nm) and UV light (390 nm) energies were transferred to and utilized in the deNO_x reaction. The light intensities of red LED (627nm), green LED (530nm), blue LED (445nm), and UV LED (390nm) were 62.76, 125.12, 76.22, and 73.70 μmol m^{-2} s^{-1}, respectively. The photoefficiency (PE) and quantum effiency (QE) can be calculated using the following equations (eqs 1 and 2), which take into account the deNO_x abilities and average absorption ratios of various light wavelengths ($\lambda = 627$ nm, $\lambda = 530$ nm, $\lambda = 445$ nm, $\lambda = 390$ nm) (Figure 3).

$$PE_\lambda = \frac{F_{NO} a_\lambda}{P_\lambda S} \times 100\% \quad (1)$$

$$QE_\lambda = \frac{F_{NO} a_\lambda}{P_\lambda S A_\lambda} \times 100\% \quad (2)$$

F_{NO} (μmol s^{-1}) is the flow quantity of NO molecules in the reaction gas, α_λ (%) the deNO_x ability of the photo catalyst, P_λ (μmol m^{-2} s^{-1}) the light intensity on the surface of the sample, S (m^2) the surface area of the sample ($S = 320$ mm^2), and A_λ (%) the average light absorption ratio of the sample at different light wavelengths (see Figure 3). It is clear that although S-TiO_2 possessed the highest QE under UV light irradiation (0.5%), the Fe- and Pt-loaded samples, TiONFe and TiONPt, possessed very high QE (nearly 0.3%), even under long-wavelength light irradiation (red LED, 627 nm). In addition, TiONFe and TiONPt possessed very high PE at all wavelength ranges (Figure 5B).

Scientists agree that active oxygen species such as singlet oxygen ($^1O_2$) can be formed by exciting the band gaps of semiconductors in air and that this excitation plays an important role in photocatalytic reactions.[21,25] Metastable singlet oxygen usually possesses higher energy than ground-state triplet oxygen.[25] Singlet oxygen shows a dimol emission at 634 nm (eq 3) and a monomol emission at 1270 nm (eq 4).[26–28]

$$^1O_2 + {}^1O_2 \rightarrow 2{}^3O_2 + h\nu \text{ (634 and 703 nm)} \quad (3)$$

$$^1O_2 \rightarrow {}^3O_2 + h\nu \text{ (1270 nm)} \quad (4)$$

Scientists agree that it may be possible to monitor weak chemiluminescence in the visible light region (634 nm) using a filter to cut off the emission attributed to the carbonyl compounds.[21]

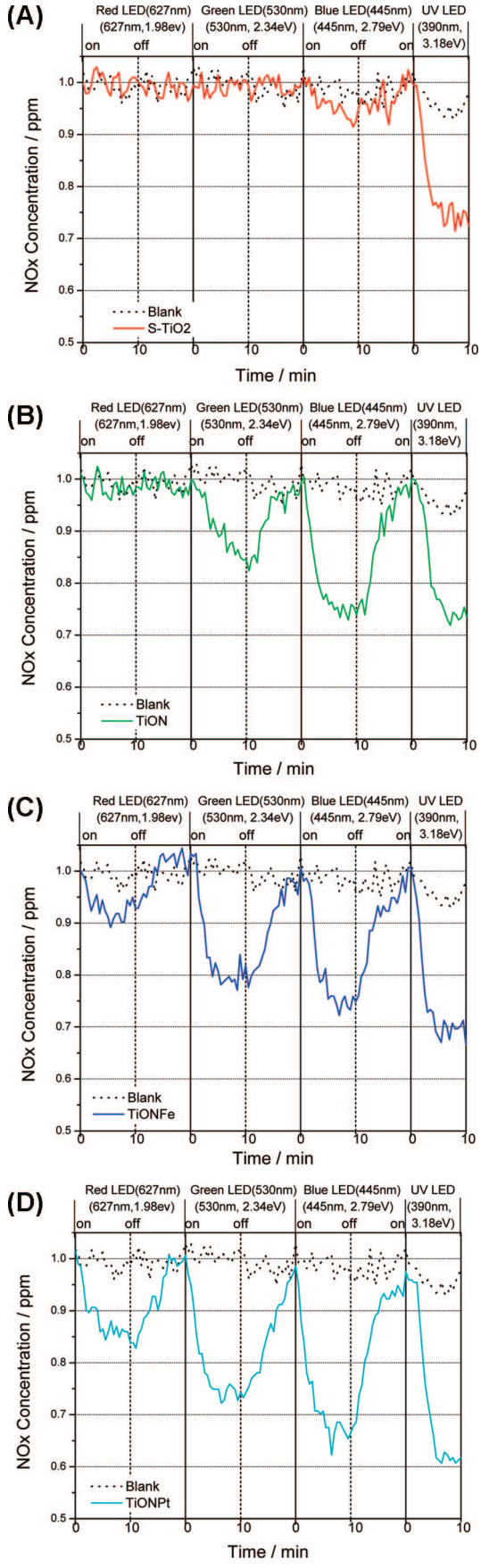

Figure 4. Irradiation time dependence of NO_x concentration as a function of sample type: (a) S- TiO_2, (b) TiON, (c) TiONFe, and (d) TiONPt. One ppm NO gas was pumped continuously through the reactor (373 cm^3). Irradiation was carried out using various LED light sources with a light intensity of 2 mW for 10 min; the light was then turned off to allow the concentration to return to 1 ppm.

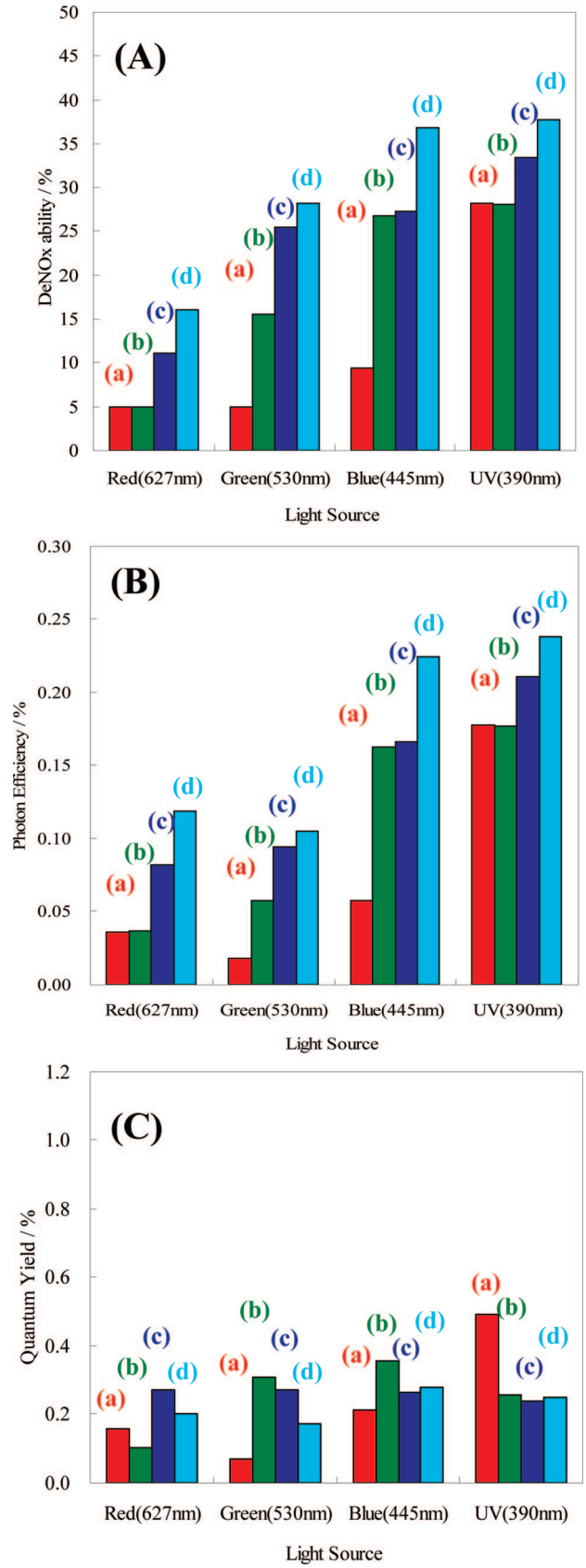

Figure 5. (A) Photocatalytic deNO$_x$ abilities, (B) photon efficiency, and (C) quantum yield of the samples (a) S-TiO_2, (b) TiON, (c) TiONFe, and (d) TiONPt under irradiation by various LED light sources.

Figures 6 and 7 show the chemiluminescence emission spectra of $^1O_2$ generated at 25 °C in air and in 1 ppm NO−50 vol % air (balanced N_2) mixed gas atmosphere by various wavelengths

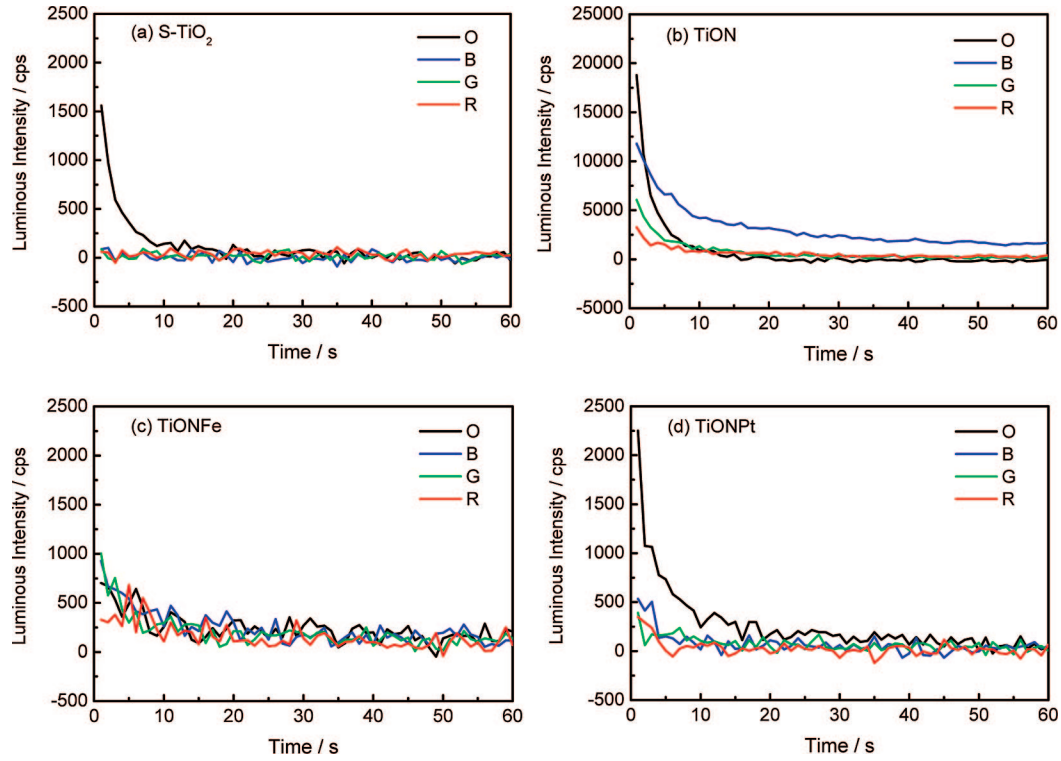

Figure 6. Chemiluminescence emission spectra of $^1O_2$ generated at 25 °C in air under irradiation by various LED light sources with different wavelengths: (a) S-TiO, (b) TiON, (c) TiONFe, (d) TiONPt. B represents blue light, G represents green light, R represents red light, and O represents UV light.

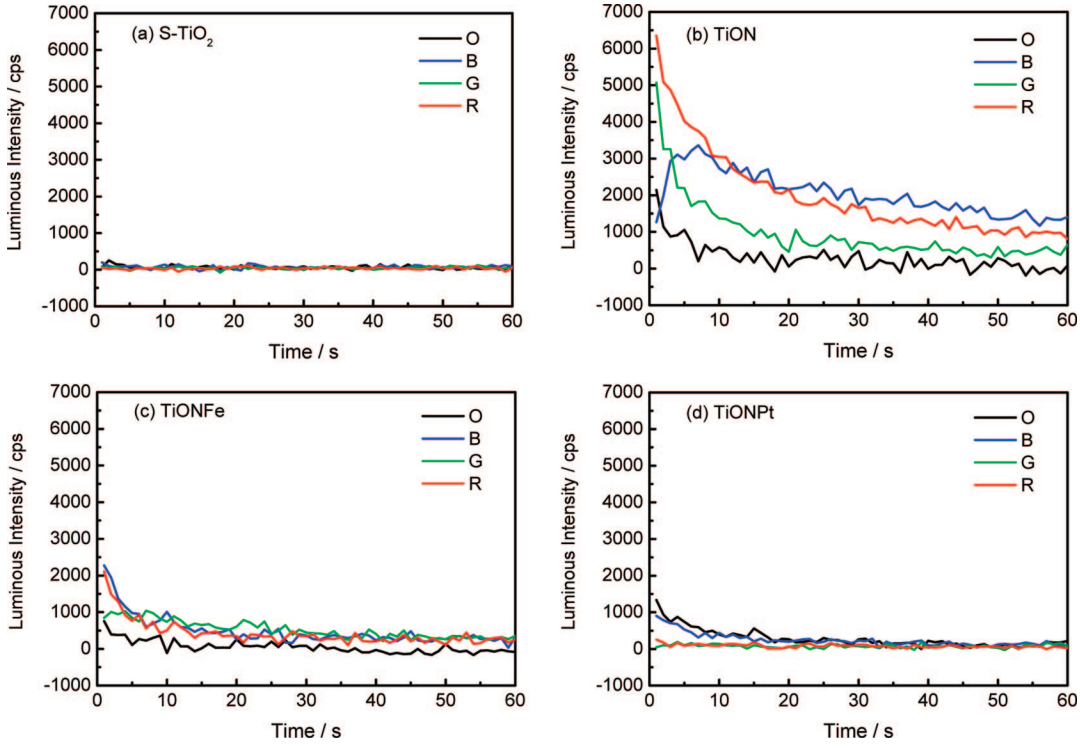

Figure 7. Chemiluminescence emission spectra of $^1O_2$ generated at 25 °C in 1 ppm NO−50 vol % air mixed (balanced N_2) gas atmosphere under irradiation by various LED light sources with different wavelengths: (a) S-TiO_2, (b) TiON, (c) TiONFe, (d) TiONPt. B represents blue light, G represents green light, R represents red light, and O represents UV light.

of UV and visible light irradiation. S-TiO_2 showed chemiluminescence under UV light irradiation (Figure 6a, curve O), but no noticeable chemiluminescence under blue, green, or red monochromatic LED lamp irradiation. These results agree with the fact that the band structure of S-TiO_2 possesses a band gap energy of 3.0 eV and can be excited only by light of wavelengths less than 413 nm. It is clear that the nitrogen-doped titania, TiON, was excited by several different LED lamps. Because of its newly formed N 2p band, situated above the O 2p band of the valence band in titania, the nitrogen-doped titania possessed a smaller bandgap and excellent visible light absorbance, and displayed chemiluminescence emission intensities

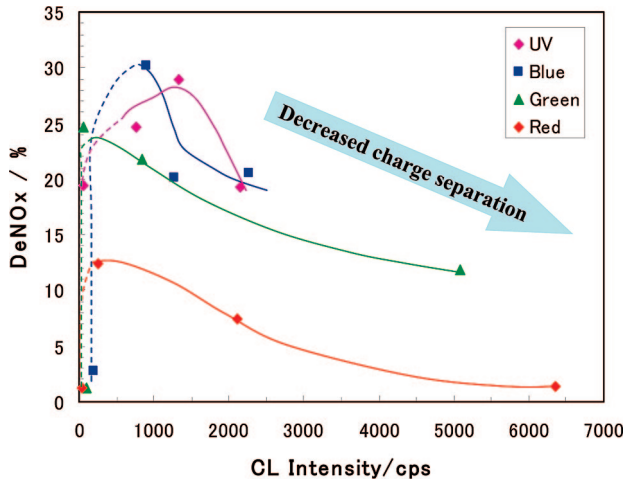

Figure 8. Relationship between chemiluminescence emission intensity and deNO$_x$ photocatalytic activity under irradiation by various LED light sources.

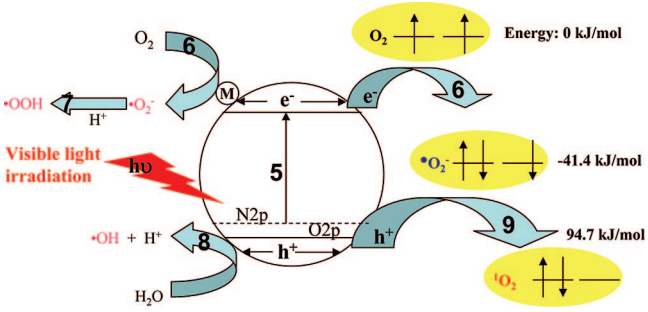

Figure 9. Schematic illustration of the photoinduced charge transformation on nitrogen doped titania with metallic loading.

for $^1O_2$ quite high compared to those of S-TiO$_2$. TiONFe and TiONPt also showed high chemiluminescence emission intensities; however, they were much lower than that of TiON. It is clear that the chemiluminescence emission spectra in air possessed intensities in descending order as follows: UV (line O), blue (line B), green (line G), and red (line R) (see Figure 6a−d). However, the spectral intensity of the samples, S-TiO$_2$ and TiON in particular, decreased significantly in the presence of NO$_x$ (Figure 7) due to the interaction between NO$_x$ and superoxide radicals, which will be explained later (eq 13). The relationship between the chemiluminescence emission intensities in an NO$_x$ atmosphere and the deNO$_x$ photocatalytic activity are summarized in Figure 8. The dotted lines indicate undoped S-TiO$_2$, and the solid lines indicate the visible light induced photocatalysts TiON, TiONFe, and TiONPt. S-TiO$_2$ showed very weak chemiluminescence emission intensities and very low visible light induced photocatalytic activity, for reasons relating to its large band gap. For the other visible light induced photocatalysts, TiON, TiONFe, and TiONPt, it is clear from the data that deNO$_x$ ability decreased with an increase in chemiluminescence emission intensity. The photocatalytic deNO$_x$ activity of TiON was at almost the same level as that of S-TiO$_2$ under UV and red LED (627 nm) irradiation, and showed higher values than those of S-TiO$_2$ under visible blue and green LED irradiation, but lower values than those of the Fe- or Pt-loaded samples under every type of LED light irradiation. This may have been related to the different band structures and the existence of Fe and Pt loaded onto the surface of the TiON. Electron/hole pairs are formed by the photoexcitation of titania (eq 5). In the presence of oxygen, these photoinduced electrons are immediately trapped by the molecular oxygen to form $\bullet O_2^-$ (eq 6), which can then generate active •OOH radicals (eq 7).[2,22,30] At the same time, the holes are trapped by water in the air to produce hydroxyl radicals (eq 8).[2,22,30] The simple free radical, •R, is a doublet and has one unpaired electron, which possesses a low energy of −41.4 kJ/mol. The singlet oxygen, however, has a pair of electrons (one up-spin and one down-spin) in one orbital, with the second equal-energy orbital empty. Metastable singlet oxygen possessed more energy (94.7 kJ/mol) than the ground-state triplet oxygen (0 kJ/mol).[26] Holes may trap one electron from the superoxide radiacal, $\bullet O_2^-$, to produce a singlet oxygen (eq 9) or triplet oxygen (eq 10). From the energy level, it is also possible for the superoxide radical, $\bullet O_2^-$, to be produced easily and quickly, while the singlet oxygen should be formed slowly and required extended energy.

$$TiO_2 \xleftrightarrow{h\upsilon} TiO_2\,(e_{CB}^- + h_{VB}^+) \quad (5)$$

$$e_{CB}^- + O_2 \rightarrow \bullet O_2^- \quad (6)$$

$$\bullet O_2^- + H^+ \rightarrow \bullet OOH \quad (7)$$

$$h_{VB}^+ + H_2O \rightarrow \bullet OH + H^+ \quad (8)$$

$$\bullet O_2^- + h_{VB}^+ \rightarrow {}^1O_2 \quad (9)$$

$$\bullet O_2^- + h_{VB}^+ \rightarrow {}^3O_2 \quad (10)$$

The formation of singlet oxygen $^1O_2$ (eq 9) competed with that of superoxide radicals and hydroxyl radicals (eqs 6, 7). It is clear that Fe and Pt loading increased the charge transfer and charge separation on the surface of the photocatalysts.

Figure 9 shows a schematic illustration of photoinduced charge transfer on Fe- and Pt-loaded, nitrogen-doped titania. The formation processes for the radicals and singlet oxygen are detailed in the previously mentioned equations. Singlet oxygen $^1O_2$ may be formed by the electron−hole recombination process shown in eqs 6 and 9. In the case of Fe and Pt loading on photocatalyst surfaces, the photoinduced electrons transformed rapidly on the surface of the Fe and Pt to depress electron−hole recombination. As a result, because of the promoted charge transfer on the photocatalyst surface, Fe- and Pt-loaded TiON prefer to produce more superoxide and hydroxyl radicals.[30−32] In other words, the electrons and superoxide radicals on the surface of iron or platinum resisted recombination with holes on the valence band of the titania surface, which would have produced singlet oxygens and/or triplet oxygen; it is important to remember that the iron or platinum particles were separated from the surface of the TiON. As a result, if photocatalysts can be induced by various wavelengths of light, the solid lines in Figure 8 may contribute to the characterization of charge separation behavior.

The deNO$_x$ reaction reportedly relates to oxidation through active oxygen species, such as •OH and $\bullet O_2^-$. These reactions are displayed in eqs 11–13.[33,34] Nitrogen monoxide reacted with these reactive radicals, molecular oxygen, and a very small amount of water in the air (humidity was about 25% in the present study) to produce HNO$_2$ or HNO$_3$. It has also been reported that about 20% of the nitrogen monoxide decomposed directly into nitrogen and oxygen.[34]

$$NO + 2\bullet OH \rightarrow NO_2 + H_2O \quad (11)$$

$$NO_2 + \bullet OH \rightarrow NO_3^- + H^+ \quad (12)$$

$$NO_x + \bullet O_2^- \rightarrow NO_3^- \quad (13)$$

In the NO_x atmosphere, the NO_x molecule may have trapped the superoxide radical $\bullet O_2^-$ to form NO_3^- (eq 13). As a result, the NO_x molecule consumed the superoxide radical $\bullet O_2^-$ and delayed the singlet oxygen formation reaction (eq 9), therefore causing the chemiluminescence emission spectra intensity in the NO atmosphere (Figure 7) to be much lower than those in air.

Summary

In summary, the following conclusions have been drawn:

1. Nanosized titania showed very low deNO_x ability under visible light irradiation, in spite of their excellent UV light induced ($\lambda = 390$ nm) deNO_x ability.

2. Nitrogen-doped titania possessed excellent photocatalytic activity under visible light irradiation of $\lambda = 445$ nm and $\lambda = 530$ nm.

3. Fe and Pt loading improved the photocatalytic activity of nitrogen-doped titania under not only UV light but also long-wavelength visible light irradiation ($\lambda = 530$ nm and $\lambda = 627$ nm).

4. Pt-loaded, nitrogen-doped titania possessed the best visible light and UV light induced photocatalytic activity. In addition, Fe- and Pt-loaded, nitrogen-doped titania possessed a high quantum yield under long-wavelength light LED lamp irradiation.

Acknowledgment. This research was carried out as one of the projects under the Special Education and Research Expenses on "Post-Silicon Materials and Devices Research Alliance" and the JSPS Asian Core Program "Interdisciplinary Science of Nanomaterials ", JSPS Core University Program (CUP), and a Grant-in-Aid for Science Research (20360293).

References and Notes

(1) Test method for air purification performance of photocatalytic materials - Part 1: Removal of nitric oxide, Japanese Standards Association. *Japanese Industrial Standard (JIS R 1701−1:2004(J))*; Established on 2004−01−20.

(2) Yin, S.; Sato, T. Synthesis and photocatalytic properties of fibrous titania prepared from protonic layered tetratitanate precursor in supercritical alcohols. *Ind. Eng. Chem. Res.* **2000**, *39*, 4526–4530.

(3) Yin, S.; Hasegawa, H.; Maeda, D.; Ishitsuka, M.; Sato, T. Synthesis of visible-light-active nanosize rutile titania photocatalyst by low temperature dissolution-reprecipitation process. *J. Photochem.Photobiol., A* **2004**, *163*, 1–8.

(4) Yin, S.; Sato, T. Synthesis of high-active photocatalyst by soft chemical processes. *Recent Res. Dev. Solid State Ionics* **2004**, *2*, 33–70.

(5) Asahi, R.; Morikawa, T.; Ohwaki, T.; Aoki, K.; Taga, Y. Visible-light photocatalysis in nitrogen-doped titanium oxides. *Science* **2001**, *293*, 269–271.

(6) Morikawa, T.; Asahi, R.; Ohwaki, T.; Aoki, K.; Taga, Y. Band-gap narrowing of titanium dioxide by nitrogen doping. *Jpn. J. Appl. Phys.* **2001**, *40*, L561–L563.

(7) Justicia, I.; Ordejon, P.; Canto, G. Designed self-doping titanium oxide thin films for efficient visible-light photocatalysis. *Adv. Mater.* **2002**, *14*, 1399–1402.

(8) Khan, S. U. M.; Al-Shahry, M.; Ingler, W. B., Jr. Efficient photochemical water splitting by a chemically modified n-TiO_2. *Science* **2002**, *297*, 2243–2245.

(9) Umebayashi, T.; Yamaki, T.; Itoh, H,.; Asai, K. Band-gap narrowing of titanium dioxide by sulfur doping. *Appl. Phys. Lett.* **2002**, *81*, 454–456.

(10) Yin, S.; Zhang, Q.; Saito, F.; Sato, T. Preparation of visible-light active titania photocatalyst by mechanochemical method. *Chem. Lett.* **2003**, *32*, 358–359.

(11) Wang, J.; Yin, S.; Zhang, Q.; Saito, F.; Sato, T. Mechanochemical synthesis of $SrTiO_{3-x}F_x$ with high visible light photocatalytic activities for nitrogen monoxide destruction. *J. Mater. Chem.* **2003**, *13*, 2348–2352.

(12) Irie, H.; Watanabe, Y.; Hashimoto, K. Carbon-doped anatase TiO_2 powders as a visible-light sensitive photocatalyst. *Chem. Lett.* **2003**, *32*, 772–773.

(13) Zhang, Q.; Wang, J.; Yin, S.; Sato, T.; Saito, F. Synthesis of a visible-light active $TiO_{2-x}S_x$ photocatalyst by means of mechanochemical doping. *J. Am. Ceram. Soc.* **2004**, *87*, 1161–1163.

(14) Yin, S.; Aita, Y.; Komatsu, M.; Wang, J.; Tang, Q.; Sato, T. Synthesis of excellent visible-light responsive $TiO_{2-x}N_y$ phoyocatalyst by a homegeneous precipitation-solvothermal process. *J. Mater. Chem.* **2005**, *15*, 674–682.

(15) Li, D.; Haneda, H.; Labhsetwar, N. K.; Hishita, S.; Ohashi, N. Visible-light-driven photocatalysis on flurine-doped TiO_2 powders by the creation of surface oxygen vacancies. *Chem. Phys. Lett.* **2005**, *401*, 579–584.

(16) Yin, S.; Komatsu, M.; Zhang, Q.; Saito, F.; Sato, T. Synthesis of visible-light responsive nitrogen/carbon doped titania photocatalyst by mechanochemical doping. *J. Mater. Sci.* **2007**, *42*, 2399–2403.

(17) Morikawa, T.; Irokawa, Y.; Ohwaki, T. Enhanced photocatalytic activity of $TiO_{2-x}N_x$ loaded with copper ions under visible light irradiation. *Appl. Catal., A* **2006**, *314*, 123–127.

(18) Ohno, T.; Miyamoto, Z.; Nishijima, K.; Kanemitsu, H.; Xueyuan, F. Sensitization of photocatalytic activity of S- or N-doped TiO_2 particles by adsorbing Fe^{3+} cations. *Appl. Catal., A* **2006**, *302*, 62–68.

(19) Morikawa, T.; Ohwaki, T.; Suzuki, K.; Moribe, S.; Tero-Kubota, S. Visible-light-induced photocatalytic oxidation of carboxylic acids and aldehydes over N-doped TiO_2 loaded with Fe, Cu or Pt. *Appl. Catal., B* **2008**, *83*, 56–62.

(20) Gateshki, M.; Yin, S.; Ren, Y.; Petkov, V. Titania polymorphs by soft chemistry: is there a common structural pattern? *Chem. Mater.* **2007**, *19*, 2512–2518.

(21) Nosaka, Y.; Daimon, T.; Nosaka, A. Y.; Murakami, Y. Singlet oxygen formation in photocatalytic TiO_2 aqueous suspension. *Phys. Chem. Chem. Phys.* **2004**, *6*, 2917–2918.

(22) Hoffmann, M. R.; Martin, S. T.; Choi, W.; Bahnemann, D. W. Environmental applications of semiconductor photocatalysis. *Chem. Rev.* **1995**, *95*, 69–96.

(23) Fujishima, A.; Rao, T. N.; Tryk, D. A. Titanium dioxide photocatalysis. *J. Photochem. Photobiol., C* **2000**, *1*, 1–21.

(24) Maldotti, A.; Molinari, A.; Amadelli, R. Photocatalysis with organized systems for the oxofunctionalization of hydrocarbons by O^-_2. *Chem. Rev.* **2002**, *102*, 3811–3836.

(25) Kearns, D. R. Physical and chemical properties of singlet molecular oxygen. *Chem. Rev.* **1971**, *71*, 395–427.

(26) Kanofsky, J. R. Singlet oxygen production by biological systems. *Chem. Biol. Interact.* **1989**, *70*, 1–28.

(27) Miyazawa, T.; Fujimoto, K.; Kinoshita, M.; Usuki, R. Rapid estimation of peroxide content of soybean oil by measuring thermoluminescence. *J. Am. Oil Chem. Soc.* **1994**, *71*, 343–344.

(28) Mulliken, R. S. Interpretation of the atmospheric oxygen bands; electronic levels of the oxygen molecule. *Nature* **1928**, *122*, 505.

(29) Gerischer, H.; Heller, A. The role of oxygen in photooxidation of organic molecules on semiconductor particles. *J. Phys. Chem.* **1991**, *95*, 5261–5267.

(30) Cozzoli, P. D.; Fanizza, E.; Comparelli, R.; Curri, M. L.; Agostiano, A. Role of metal nanoparticles in TiO_2/Ag nanocomposite-based microheterogeneous photocatalysis. *J. Phys. Chem. B* **2004**, *108*, 9623–9630.

(31) Tian, Y.; Tatsuma, T. Mechanisms and applications of plasmon-induced charge separation at TiO_2 films loaded with gold nanoparticles. *J. Am. Chem. Soc.* **2005**, *127*, 7632–7637.

(32) Zou, J.; Liu, C.; Zhang, Y. Control of the metal-support interface of NiO-loaded photocatalysts via cold plasma treatment. *Langmuir* **2006**, *22*, 2334–2339.

(33) Dalton, J. S.; Janes, P. A.; Jones, N. G.; Nicholson, J. A.; Halam, K. R.; Allen, G. C. Photocatalytic oxidation of NOx gases using TiO_2: a surface spectroscopic approach. *Environ. Pollut.* **2002**, *120*, 415–422.

(34) Anpo, M. In *Recent Developments on Visible Light Response Type Photocatalysts*; NTS: Tokyo, 2002; p 9.

JP803371S